New Phytol. (1999), **143**, 351–364

Exploring the relationships between reflectance and anatomical and biochemical properties in *Quercus ilex* leaves

J. M. OURCIVAL, R. JOFFRE* AND S. RAMBAL

Centre d'Ecologie Fonctionnelle et Evolutive, CNRS, 1919 Route de Mende, 34293 Montpellier Cedex 5, France

Received 13 November 1998; accepted 16 March 1999

SUMMARY

Leaf anatomical parameters such as leaf mass per area (LMA) and biochemical composition can be used as indicators of leaf photosynthetic capacity. The aims of this study are to evaluate the potential of reflectance spectroscopy of fresh leaves for assessing and predicting various parameters, anatomical (LMA and tissue thickness) and biochemical (nitrogen concentration). This paper describes results obtained with fresh leaves of holm oak (*Quercus ilex*), an evergreen oak that is widely distributed from mesic to xeric habitats in the Mediterranean. Fresh leaves (560) were collected over 3 yr at six different sites, from the top to the bottom of the canopy. The reflectance of each leaf was obtained within 1 h of sampling with an NIRSystems 6500 spectrophotometer over the range 400–2500 nm. LMA was determined for all samples; biochemical and anatomical measurements were conducted over representative subsample populations of 92 and 87 leaves, respectively. Stepwise regression calibrations and partial least squares (PLS) calibrations were developed and compared with different spectral regions and mathematical treatments. Calibration equations had high coefficients of determination (r^2 ranging from 0.94 for nitrogen to 0.98 for LMA and tissue thickness). The PLS regressions gave better results than stepwise regressions for all parameters studied. Compared with regressions calculated on raw spectral data, calculations on second derivatives of spectra improved results in all cases. The use of scatter corrections also improved results. These results show that visible and near-infra red reflectance can be used for accurately predicting anatomical parameters and the nitrogen concentration of fresh holm oak leaves. The results support the suggestion that high spectral resolution imaging spectrometry can be a useful tool for assessing functional processes in forest ecosystems.

Key words: anatomy, thickness, leaf mass per area, reflectance, infrared spectroscopy, *Quercus ilex*.

INTRODUCTION

Relationships between anatomical and biochemical leaf parameters and physiological plant activity have been documented at different levels of organization from the individual to the biome scale (Field, 1991). At the individual level, anatomical and functional differences among leaves from different vertical positions have been identified (Oren *et al.*, 1986; Givnish, 1988; Gutschick & Wiegel, 1988; Hollinger, 1989; Ashton & Berlyn, 1994; Rambal *et al.*, 1996). Parameters that correspond to leaf anatomy, such as leaf mass per area (LMA) and tissue thickness, are known to be influenced by leaf position within the canopy. The total thickness of leaves decreases with growth irradiance, but the thickness of the different tissues of the mesophyll (the palisade and spongy mesophyll) is reduced in variable proportions (Hanson, 1917; Turrell, 1936; Jackson, 1967). These changes are related to important photosynthetic and/or stomatal conductance modifications (Araus *et al.*, 1986; Field & Mooney, 1986; Givnish, 1988; Abrams & Kubiske, 1990, 1994; Ashton & Berlyn, 1994). Mechanistic evidence of the influence of leaf structure on photosynthesis has been obtained recently (Terashima & Hikosaka, 1995; Vogelmann *et al.*, 1996); however, Smith *et al.* (1997) point out that a comprehensive synthesis of the functional significance of leaf structure as related to photosynthesis has yet to be proposed.

Relationships between canopy average LMA and stand productivity have also been established across resource gradients (Specht & Specht, 1989; Field, 1991; Pierce *et al.*, 1994; Rambal, 1999). For Mediterranean evergreen oak forests, Rambal *et al.* (1996) have shown that changes in LMA due to variations in availability of water and nutrients are accompanied by changes in photosynthetic per-

*Author for correspondence (fax +33 4 67 41 21 38; e-mail joffre@cefe.cnrs-mop.fr).

formance. Finally, a global study carried out by Reich *et al.* (1997) on six biomes, ranging from deserts to tropical forests, showed that relationships between leaf structure and function and plant growth appear to conform to a general pattern, whatever the biome studied. These authors showed for a group of 280 plant species that an increase in photosynthesis and respiration is linked to a rise in leaf N concentration and specific leaf area, and, at the same time, to a reduction of leaf life span. Together these results, obtained over a range of organizational levels, suggest that a certain number of leaf parameters, such as LMA or N concentration, are important indicators of plant physiological function. The results also suggest that these parameters contribute significantly to regulation processes all the way from the leaf through to the ecosystem and biome levels. Moreover, measures of foliar N concentration provide us not only with indicators of plant productivity, but also with information on some aspects of litter decomposition and nutrient availability (Wessman *et al.*, 1988; Curran, 1989). Therefore estimates of anatomical and biochemical parameters of leaves derived from reflectance data give spatial and scale perspectives that could be useful in predicting photosynthetic capacity and nutrient cycling parameters for terrestrial ecosystems.

Reflectance of dried, ground samples in the 1100–2500 nm region (referred to as the NIR region) is widely used to determine plant biochemical composition (Norris *et al.*, 1976; Card *et al.*, 1988; McLellan *et al.*, 1991; Meuret *et al.*, 1993; Damesin *et al.*, 1997; Foley *et al.*, 1998). The possible application of reflectance spectroscopy for analysing biochemical composition of fresh plant material has been recently investigated in the 400–2500 nm spectral domain, both at leaf level (Curran *et al.*, 1992; Lacaze & Joffre, 1994; Martin & Aber, 1994; Grossman *et al.*, 1996) and at canopy level (Wessman *et al.*, 1988, 1989; Johnson *et al.*, 1994), with contrasting results. Spectral analysis of fresh leaves is complicated for two major reasons. First, reflectance spectra of fresh leaves in the 400–2500 nm spectral domain are remarkably similar between species and environments, due to dominant features related to absorption by photosynthetic pigments (visible) and water (near- and mid-infra red (IR)). The main features in the near- and the mid-IR correspond to four major absorption peaks of water at *c.* 975, 1175, 1450 and 1930 nm. Secondly, a layer of wax on the upper side of the leaf may actually cause a high specular reflectance (Vanderbilt *et al.*, 1985).

This study tests the hypothesis that spectral information on fresh leaves contains not only information about leaf biochemical composition, but also information about leaf anatomy, which could tell us more about how plants work. The predictive relationships between spectra and anatomy and/or biochemistry cannot be based solely on causal explanations, because chemical and physical interferences introduce noise in the reflectance signal obtained from intact, fresh leaves. An empirical calibration approach based on chemometric methods is used to concentrate the relevant information from spectral and measured data into simplified synthetic maps that give good statistical predictions of biochemical and anatomical parameters (Martens & Naes, 1989).

The objectives of this study were: to establish relationships between different anatomical and biochemical leaf parameters; to determine variation of spectral reflectance in fresh leaves with relation to these parameters; and to explore the possibility of establishing predictive relationships between leaf parameters and spectral data. This paper outlines results obtained with fresh leaves of holm oak (*Quercus ilex*), a widespread evergreen Mediterranean oak that occurs in mesic through to xeric habitats and presents a strong adaptability of leaves to wide ranges of light inputs (Rambal *et al.*, 1996; Castro Diéz *et al.*, 1997; Damesin *et al.*, 1997).

MATERIALS AND METHODS

Sample collection

Leaves of the evergreen holm oak *Quercus ilex* L. usually remain on shoots for >1 yr. The leaves are extremely variable in size (ranging from 3 to 25 cm^2) and shape (dentate or entire, sub-lobate with an acute tip, or obtuse). The leaves are densely pubescent on the underside. A total of 560 leaves were collected on nine different dates in 1994–96, at six different sites located <30 km from Montpellier, France. To sample a representative set of different types of leaves, branches were harvested at various levels ranging from the upper to the lower position in the canopy. Branches 40 cm in length were placed in refrigerated plastic bags with damp towels until spectroscopic measurements were made. For each branch, only mature, current-year leaves were used.

Spectroscopic measurements

An NIRSystems Model 6500 spectrophotometer (NIR Systems, Silver Spring, MD, USA) was used to gather reflectance spectra of fresh leaves. This instrument has a spectral range of 400–2500 nm, with 2 nm sampling intervals. The bandwidth was 10 nm and the wavelength accuracy ± 0.5 nm. The incident beam is normal to the target. Reflected radiance is measured at a 45° angle, allowing any effect of specular light to be ignored. For each measurement, 32 scans were made to produce a mean spectrum with 1050 data points. The spectrum of apparent reflectance R is evaluated by internal software relative to a ceramic standard. The software further processes the data and records it as ab-

sorbance units (A) equal to log $1/R$ (Shenk & Westerhaus, 1991b). All samples were scanned within 1 h of removal from the branches. Laboratory-built black delrin spectrophotometric cells, with 26-mm-diameter glassless windows, were used. The absorbance relative to the adaxial surface of each leaf was measured, with a titanium dioxide-doped ceramic disk as white background.

Biochemical and anatomical measurements

After the acquisition of spectra, several anatomical and biochemical measurements were made. LMA was determined for the 560 leaves. Leaf area was measured using a leaf area meter (Delta-T Image Analysis System, Delta-T Devices, Cambridge, UK). The dry mass was determined after drying for 48 h in an oven at 60°C. A subsample of 92 leaves was selected based on the spectral variability (see later) and the corresponding leaves were ground (vibrogrinder MM 2000 Retsch) and N concentration determined with a Perkin-Elmer elemental analyser (PE 2400 CHN).

Anatomical measurements were conducted in April 1996 on 87 leaves sampled from 28 trees from three of the six study sites. Each leaf was hand-sectioned from the middle portion of the lamina across the central vein. Three replicates for each leaf were mounted in distilled water and observed immediately, without staining, under a light microscope (Olympus CH-2, ×400). The thickness of the tissues, cuticle, upper epidermis, palisade mesophyll and spongy mesophyll, was determined with an ocular micrometer.

Spectral data processing

Two objectives were followed: the optimization of sample choice for chemical analysis (N concentration) to obtain a representative set of data encompassing the total variability; and the establishment of predictive relationships between spectral, anatomical and biochemical data. For complex analytical problems with noise inherent in the system, the parameters must be estimated statistically, based on realistic, empirical measurements from representative calibration samples (Martens & Naes, 1989).

Sample selection procedure

A principal components analysis (PCA) was performed on the 560 spectra to identify and eliminate samples that deviated too far from the sample mean and to select a subsample population for wet chemistry analysis. The spectra were first derivatized to emphasize small absorption peaks and to remove baseline shifts (Hruschka, 1987; Shenk & Westerhaus, 1991a, b). Mahalanobis distances, H (Mahalanobis, 1936) from the average spectrum were then computed on the sample loadings. This procedure provides a ranking of the spectral data on the basis of the standardized H distance. During a calibration it was generally assumed that the samples with spectra of a standardized H value greater than three were outliers compared to the population (Shenk & Westerhaus, 1991b). Two samples in 560 had an H distance greater than three: they were therefore considered to be outliers, and were eliminated. For the remaining samples, selection of samples for chemical analysis was done by analysing the distance matrix formed, using Mahalanobis distances between all pairs of spectra (SELECT procedure of ISI software, see Shenk & Westerhaus, 1991a).

Calibration procedures

Research on predictive relationships between spectral, anatomical and biochemical data forces the differentiation of the sample set into two separate sets for calibration and validation. Consequently, for each variable the data set was split into a calibration set containing two-thirds of the samples, and a validation set containing one-third of the samples over which the calibration equations were applied to obtain a standard error of prediction (SEP). Stepwise regression calibrations and partial least squares (PLS) calibrations were developed and compared for N, LMA and all anatomical variables. For each regression 18 models, representing three pretreatments × transformations × three spectral regions, were applied to the data. The three pretreatments correspond to no pretreatment, standard normal variate (SNV) and de-trending transformation (Barnes *et al.*, 1989). Pretreatment of the spectra by calculation of the SNV transformation removes slope variation on an individual sample basis. De-trending accounts for the variation in baseline shift and curvilinearity with the use of a second-degree polynomial regression. The two transformations applied correspond to raw absorbance data and second-order derivative. In addition, three series of calibrations using different spectral regions were produced, the first on the entire spectrum (400–2500 nm), the second on the near-IR (1100–2500 nm), and the third on the visible and near-near-IR (400–1100 nm).

Stepwise regression is performed by selecting the wavelength that is most highly correlated with the reference values, and adding it to the equation. The second wavelength is added by calculating partial correlations with all other wavelengths and selecting the wavelength with the highest partial correlation. The process continues until the addition of a wavelength makes no further improvement to the explanation of variation in the reference value (F value significant at 0.01). After each wavelength is added to the equation, the program re-evaluates all wavelengths in the equation before continuing (Windham *et al.*, 1989; Shenk & Westerhaus, 1991a).

To avoid overfitting, the number of selected wavelengths was limited to five.

The PLS method (Martens & Jensen, 1982; Shenk & Westerhaus, 1991b) uses all the spectral information, unlike the stepwise regression method which uses only a small number of wavelengths (Windham *et al.*, 1989). PLS is the combination of PCA and multiple linear regression (MLR). By reducing the large set of raw spectral data into a small number of orthogonal factors, PLS avoids problems of overfitting and collinearity (see Martens & Naes, 1989, for a comprehensive account of multivariate calibration in spectroscopy).

RESULTS

Leaf mass per area, anatomical and biochemical parameters

Over the 560 leaves, LMA varied from 85–268 g m^{-2} (Table 1) with a coefficient of variation (CV = 100SD/mean) of 25. Total leaf thickness showed a lower range of variation from 136 to 307 μm with a CV of 19. Cuticle thickness was nearly constant and equal to 8.2 ± 2.0 μm. This value was added to that of the upper epidermis (Table 1). Among the different tissues, palisade mesophyll showed a greater coefficient of variation (32) than the others (epidermis plus cuticle 20; spongy mesophyll 16; total thickness 19). There was no significant correlation between spongy mesophyll thickness and either palisade mesophyll, or epidermis plus cuticle. In contrast, palisade mesophyll thickness was correlated with epidermis plus cuticle ($r^2 = 0.33$, $P < 0.01$). Variation of the total thickness of the leaves was mainly explained by variation of palisade mesophyll (62 % of the variance), and by variation of the upper epidermis (17 % of the variance). Palisade mesophyll showed three layers of cells in the thickest leaves, and one layer in the thinnest. Mass-based N concentration varied from 9 to 18 mg g^{-1} and was not correlated with LMA.

Correlations between anatomical parameters, nitrogen and reflectance spectra

The raw apparent reflectance spectra of the 87 leaves selected for tissue thickness measurements showed very large differences from one sample to another in all spectral domains (Fig. 1). The overall shape of the spectra is similar for all leaves, with the main spectral features corresponding to pigments (centred at 465 and 670 nm) and water (centred at 1175, 1450 and 1930 nm). The highest range of values for reflectance is observed in the 800–1300, 1500–1900 and 2000–2400 nm domains, whereas the range of reflectance in the visible domain is less important.

Due to the low variations of epidermis plus cuticle and spongy mesophyll in all the leaves studied, the correlations between spectra and these variables were not statistically significant. The variations in these tissues explain only a low part (< 20 %) of the variance of total thickness. Conversely, palisade mesophyll and total thickness were strongly correlated with reflectance spectra. Because these correlations were very similar, only the correlation between palisade mesophyll thickness and reflectance spectra is presented here. Fig. 2 shows the

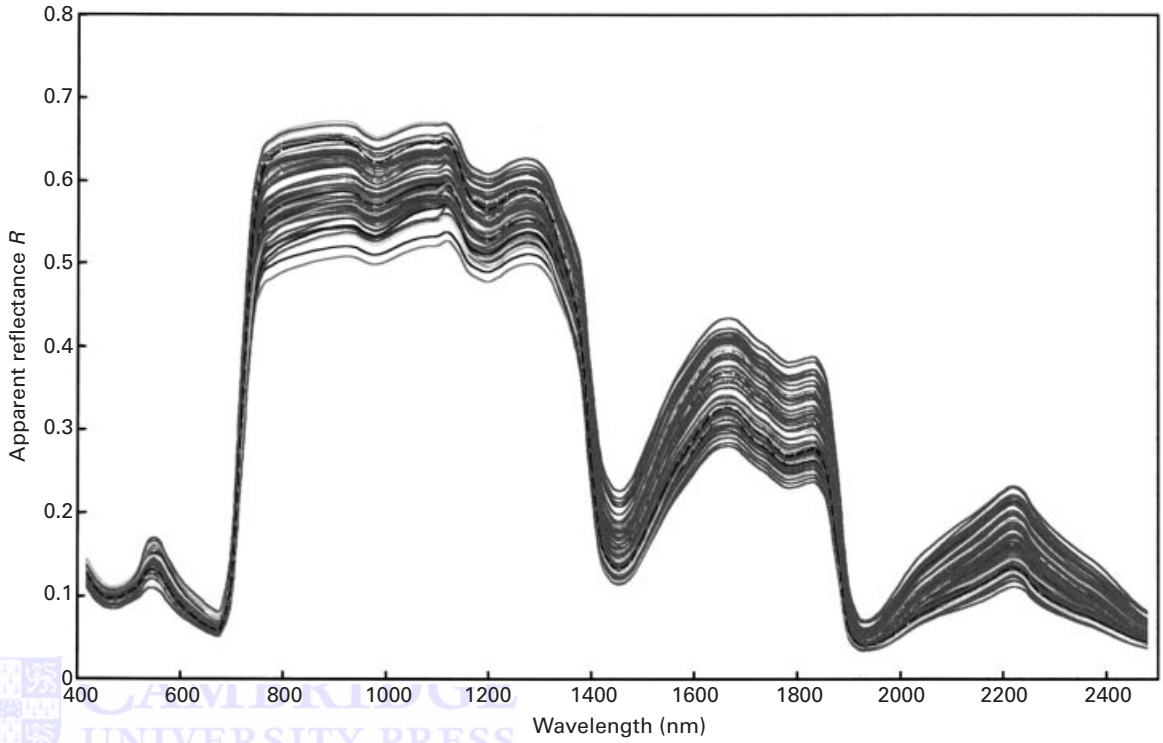

Fig. 1. Apparent reflectance spectra of the 87 *Quercus ilex* leaves analysed for anatomical measurements.

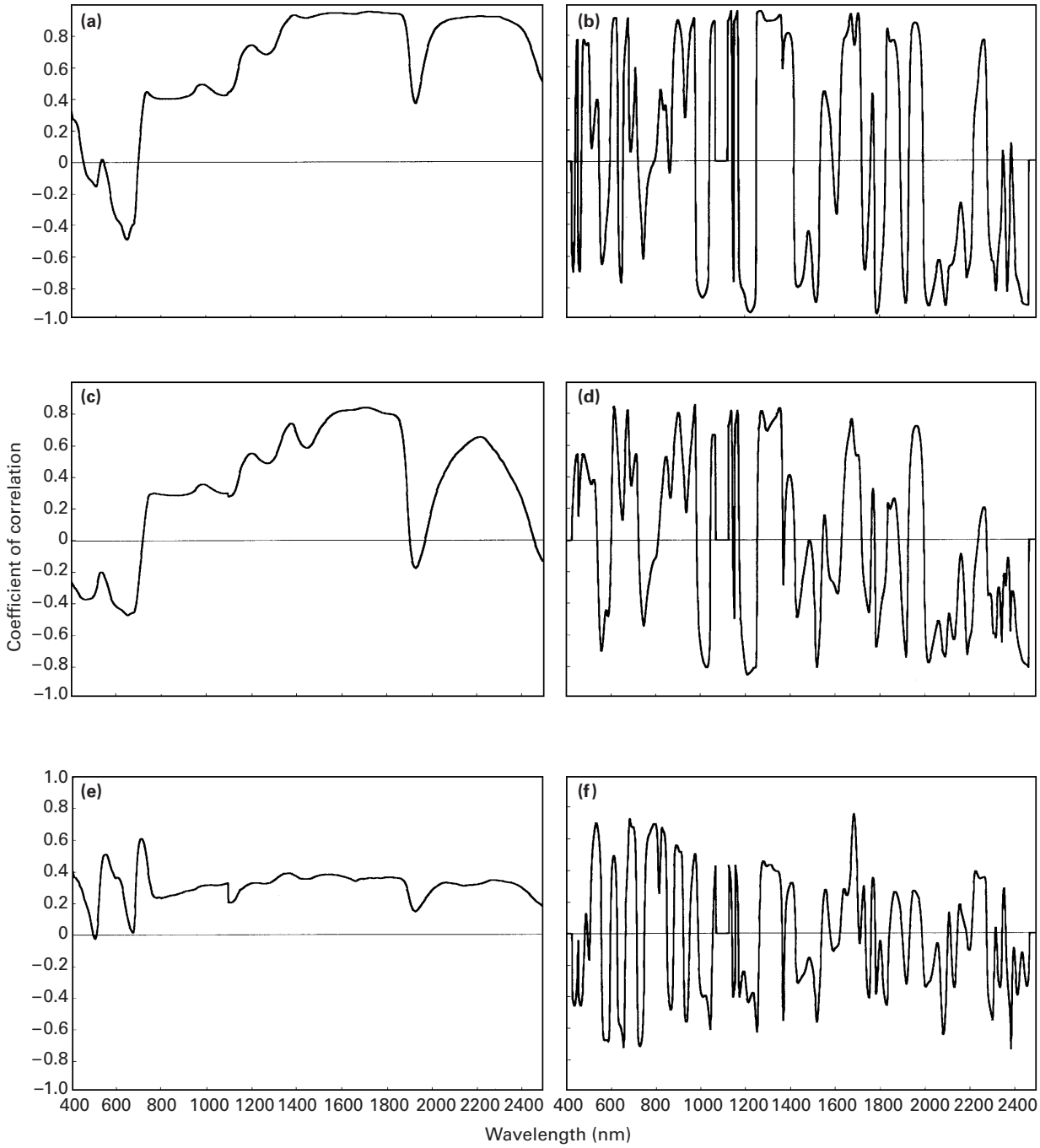

Fig. 2. Correlograms of palisade mesophyll thickness (a, b); leaf mass per area (c, d); and nitrogen concentration (e, f) with spectral data. (a, c, e) correspond to calculations made on raw spectral data; (b, d, f) to calculations made on second derivative spectra (math treatment 2, 10, 10, Table 2).

Table 1. *Biochemical and anatomical parameters of* Quercus ilex *sampled leaves*

	n	Mean	SD	CV	Min	Max
Nitrogen (mg g^{-1})	92	13.9	2.23	16	9.1	18.0
Leaf mass per area (g m^{-2})	560	179	44.3	25	84.8	268.3
Epidermis plus cuticle (μm)	87	22.2	4.45	20	15.0	35.0
Palisade mesophyll (μm)	87	111.6	35.71	32	48.9	164.9
Spongy mesophyll (μm)	87	106.4	17.4	16	66.7	154.2
Total thickness (μm)	87	239.8	44.7	19	135.7	307.4

n, sample number; SD, standard deviation; CV, coefficient of variation = 100 SD/mean.

Table 2. *Statistics for the calibration equation for palisade mesophyll thickness* (μm)

PLS regression					
Math treatment	Spectral region/ Pre-treatment	SEC	r^2	SEP	Terms
2,10,10	400–2500 nm				
	None	1.47	0.99	2.12	4
	Detrend	1.13	0.99	2.23	4
	SNV	1.46	0.99	2.04	4
	1100–2500 nm				
	None	3.27	0.99	3.78	3
	Detrend	2.70	0.99	3.20	4
	SNV	3.25	0.99	3.75	3
	400–1100 nm				
	None	7.84	0.94	9.95	2
	Detrend	5.59	0.97	10.10	4
	SNV	7.65	0.95	8.45	2
0,2,2	400–2500 nm				
	None	5.17	0.97	5.51	5
	Detrend	4.44	0.98	4.61	4
	SNV	3.33	0.99	3.32	4
	1100–2500 nm				
	None	4.00	0.98	4.52	4
	Detrend	4.54	0.98	4.46	4
	SNV	4.82	0.98	4.13	3
	400–1100 nm				
	None	12.68	0.86	14.79	3
	Detrend	8.97	0.93	12.47	4
	SNV	8.99	0.93	11.80	4

Stepwise regression					
Math treatment	Spectral region/ Pre-treatment	SEC	r^2	SEP	Wavelengths
2,10,10	400–2500 nm				
	None	4.33	0.98	4.97	1692, 1764, 1988, 2068
	Detrend	4.30	0.98	4.63	592, 1708, 1980, 2068
	SNV	3.92	0.98	4.45	648, 1364, 1660, 1916
	1100–2500 nm				
	None	4.33	0.98	4.97	1692, 1764, 1988, 2068
	Detrend	5.07	0.98	6.92	1204, 1340, 1484, 2052
	SNV	4.25	0.98	4.94	1476, 1700, 2020, 2228
	400–1100 nm				
	None	9.84	0.92	10.54	592, 976
	Detrand	7.99	0.94	9.46	592, 912, 1072
	SNV	9.90	0.91	12.23	576, 944
0,2,2	400–2500 nm				
	None	4.53	0.98	5.71	640, 696, 1668, 1684
	Detrend	4.60	0.98	4.67	1204, 1492, 2364
	SNV	5.06	0.97	5.32	1908, 2068, 2132, 2324
	1100–2500 nm				
	None	4.03	0.98	4.43	1660, 1724, 1924, 1948
	Detrend	4.26	0.98	3.79	1868, 2020, 2348
	SNV	5.06	0.97	5.32	1908, 2068, 2132, 2324
	400–1100 nm				
	None	17.07	0.76	17.83	640, 688
	Detrend	7.80	0.95	10.04	504, 600, 1000
	SNV	19.34	0.69	16.71	544, 592

Calibration sample set $n = 57$ (range 48.9–163.1; mean 112.6; SD 35.7), validation sample set $n = 30$ (range 49.4–164.9; mean 109.0; SD 36.2). Math treatment indicates the transformation of spectral data: the first number is the order of the derivative function, the second is the segments length (nm) over which the derivative was taken, and the third the segment length over which the function was smoothed. SEC, standard error of calibration; SEP, standard error of prediction. Terms, number of terms used in the PLS calibration model.

Table 3. *Statistics for the calibration equation for leaf mass per area (g m^{-2})*

PLS regression					
Math treatment	Spectral region/ Pre-treatment	SEC	r^2	SEP	Terms
2,10,10	400–2500 nm				
	None	6.57	0.98	8.34	9
	Detrend	6.76	0.98	8.54	8
	SNV	6.39	0.98	8.18	9
	1100–2500 nm				
	None	7.14	0.97	7.87	8
	Detrend	7.15	0.97	7.88	8
	SNV	7.17	0.97	8.88	9
	400–1100 nm				
	None	9.79	0.95	10.53	9
	Detrend	10.11	0.95	10.94	8
	SNV	9.45	0.95	10.56	8
0,2,2	400–2500 nm				
	None	9.53	0.95	10.65	10
	Detrend	8.34	0.96	9.22	10
	SNV	10.59	0.94	11.05	10
	1100–2500 nm				
	None	9.23	0.96	10.69	9
	Detrend	8.52	0.96	8.67	10
	SNV	11.17	0.94	11.47	10
	400–1100 nm				
	None	15.30	0.88	15.35	7
	Detrend	13.07	0.92	11.98	9
	SNV	13.30	0.92	12.37	10

Stepwise regression					
Math treatment	Spectral region/ Pre-treatment	SEC	r^2	SEP	Wavelengths
2,10,10	400–2500 nm				
	None	10.39	0.94	11.40	648, 1196, 2196, 2252, 2316
	Detrend	10.41	0.94	11.42	648, 1196, 2196, 2252, 2316
	SNV	9.13	0.96	10.26	992, 1164, 1548, 2164, 2252
	1100–2500 nm				
	None	8.46	0.96	9.17	1180, 1332, 1556, 2132, 2276
	Detrend	8.46	0.96	9.16	1180, 1332, 1556, 2132, 2276
	SNV	11.55	0.93	13.02	1180, 1212, 1236, 1516
	400–1100 nm				
	None	12.22	0.92	12.95	584, 872, 984, 1040
	Detrend	12.57	0.92	13.66	656, 872, 992, 1040
	SNV	12.07	0.92	12.52	560, 648, 992, 1040
0,2,2	400–2500 nm				
	None	10.12	0.95	10.43	1236, 1316, 1724, 2436
	Detrend	11.33	0.93	11.13	1172, 1388, 1556
	SNV	13.04	0.91	12.04	688, 1316, 1724
	1100–2500 nm				
	None	12.56	0.95	13.65	1292, 1724, 1844, 2092
	Detrend	12.36	0.92	12.48	1180, 1388, 1548
	SNV	16.85	0.84	17.85	1340, 1980, 2292
	400–1100 nm				
	None	20.32	0.79	20.37	568, 600, 616
	Detrend	23.19	0.72	23.35	528, 968
	SNV	20.57	0.78	20.70	568, 600, 616

Calibration sample set $n = 373$ (range 84.8–268.6; mean 179.3; SD 44.3), validation sample set $n = 187$ (range 84.8–265.7; mean 179.5; SD 43.8). Math treatment indicates the transformation of spectral data: the first number is the order of the derivative function, the second is the segment length (mm) over which the derivative was taken, and the third the segment length over which the function was smoothed. SEC, standard error of calibration; SEP, standard error of prediction. Terms, number of terms used in the PLS calibration model.

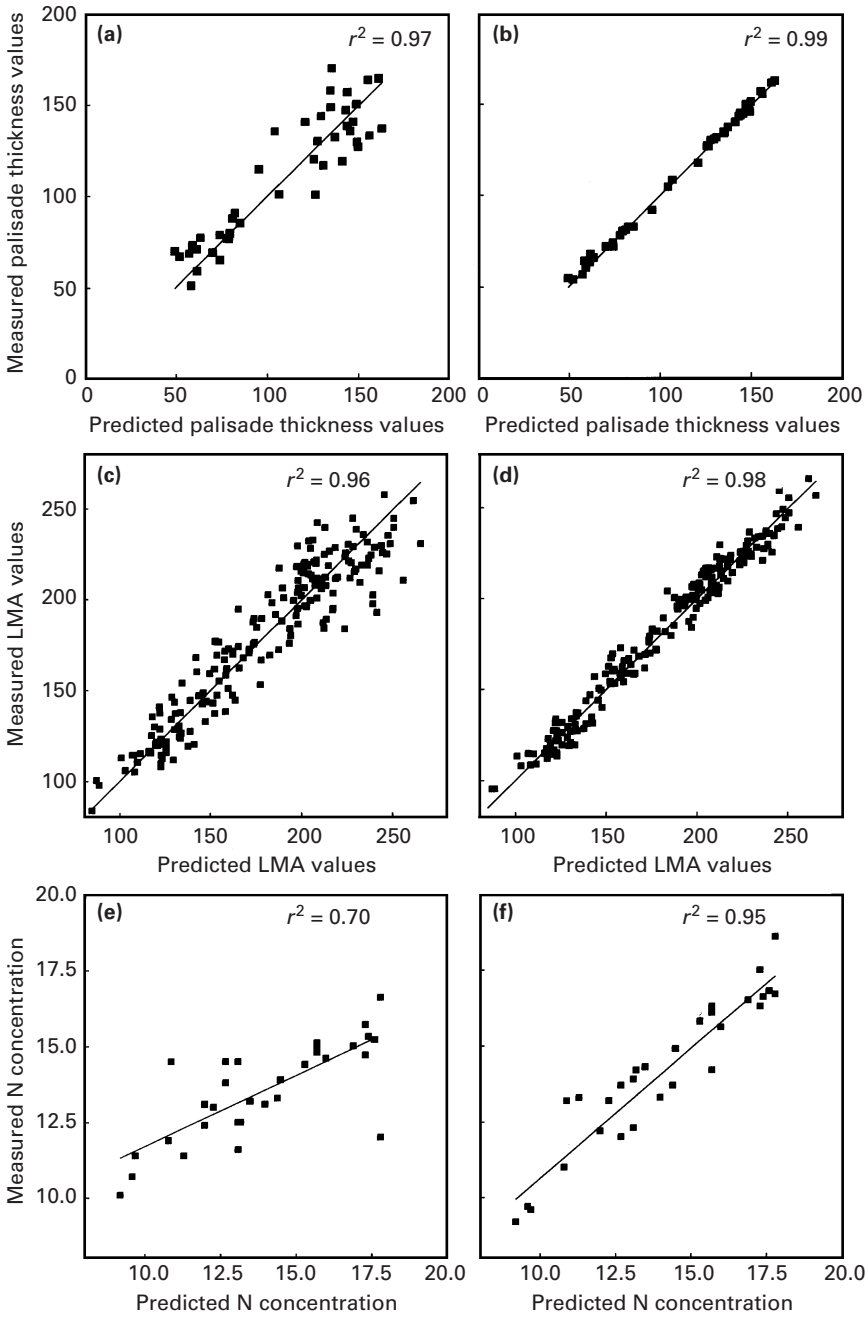

Fig. 3. Relationships between measured values and partial least squares-predicted values for palisade thickness (μm), leaf mass per area (LMA) (g m^{-2}) and nitrogen concentration (mg g^{-1}). (a, c, e) correspond to the best results obtained when calculating predictions on the raw data; (b, d, f) correspond to the best results obtained when calculating predictions on the second derivative of data.

correlations between the spectra (raw data and second derivative) and the palisade mesophyll, LMA and N. For the three parameters, spectral regions with very high correlation levels were discriminated against when using derivative treatment. In the visible region, the derivative treatment allowed a strong increase in the coefficients of correlation, particularly for the N concentration.

Calibration statistics

For the three variables, determination coefficients higher than 0.95 were obtained in at least one of the 36 calculated calibration procedures (Tables 2, 3, 4). Interestingly, whatever the mathematical treatment used, anatomical parameters (palisade mesophyll thickness and LMA) calibrated better than N concentration. For the three variables, PLS regression procedures gave better results than stepwise regression procedures (Tables 2, 3, 4). For the best combination of pre-treatments and spectral regions, the ratios between the standard error of calibration (SEC) obtained by stepwise regression and that obtained by PLS regression were 3.1, 1.5 and 1.0 for palisade mesophyll thickness, LMA, and N concentration, respectively. Whatever the PLS or step-

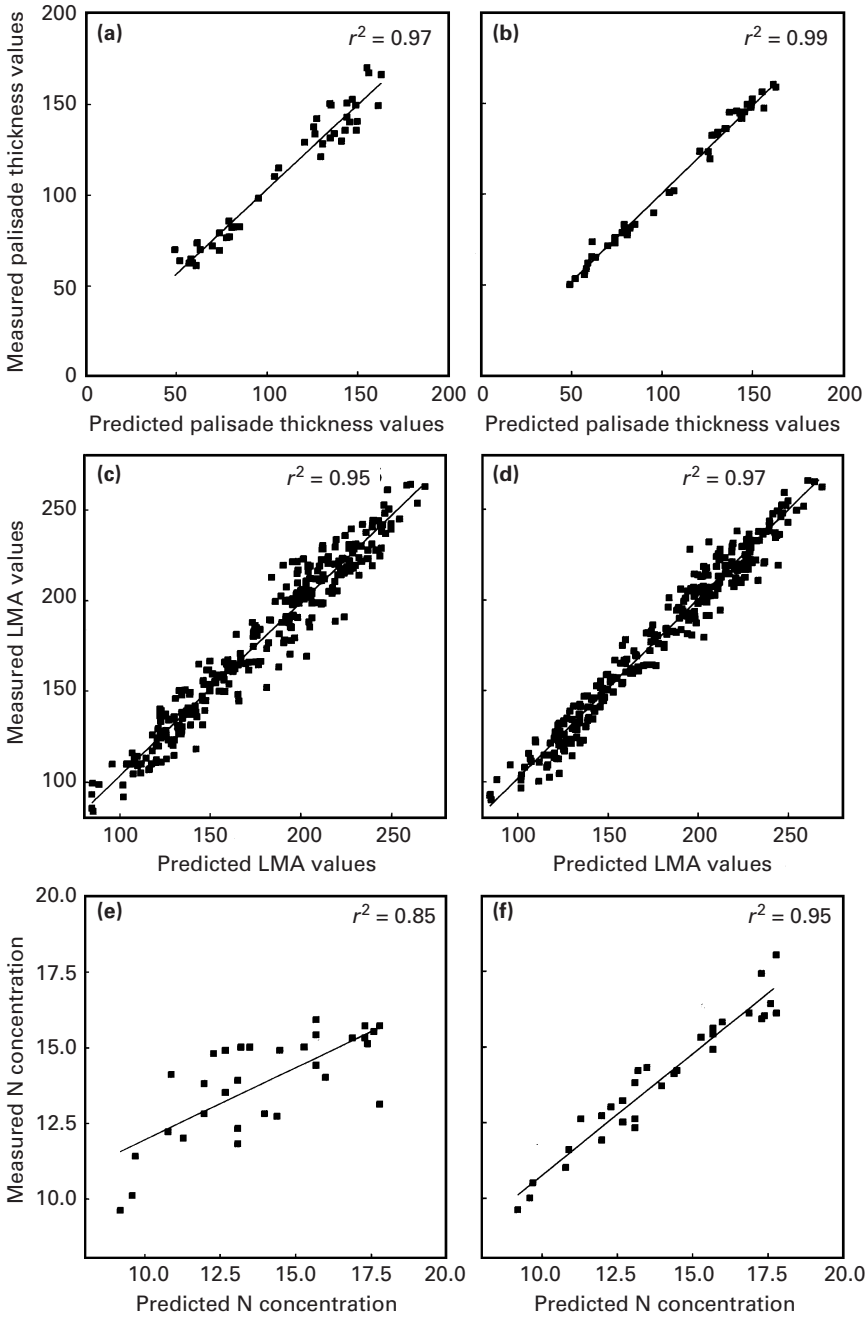

Fig. 4. Relationships between measured values and partial least squares-predicted values for palisade thickness (μm), leaf mass per area (LMA) (g m^{-2}) and nitrogen concentration (mg g^{-1}). (a, c, e) correspond to the best results obtained when calculating predictions in the 400–1100 nm region; (b, d, f) correspond to the best results obtained when calculating predictions in the 1100–2500 nm region.

wise regression methods, using the second derivative in all cases improved the results as compared to regression calculated from raw spectral data. In the same way, the ratio between SEC obtained using raw spectral data and that obtained using second derivative data were 3.2, 1.4 and 2.1 for palisade mesophyll thickness, LMA and N concentration, respectively. Fig. 3 shows the relationships between measured and predicted values for the three parameters for the best PLS regression equation obtained with raw spectra data or second derivative of spectra.

The results of prediction were almost always better when the full spectrum was taken into account, rather than just the near-IR region or the visible region. In some cases (PLS regression on raw data for palisade mesophyll, PLS regression on derivative for LMA), results obtained in the near-IR region were similar or slightly better than over the entire spectrum. By contrast, the use of the visible region alone did not allow calibration with comparable accuracy (Fig. 4). The pre-treatments (de-trend and SNV) did not significantly improve calibrations calculated over the derivative of the spectra. In

contrast, although there is no absolute trend, the pre-treatments improved the raw spectra-based calibrations.

DISCUSSION

In numerous modelling approaches for radiative transfers within plant canopies and associated carbon and water exchanges, the canopy is stratified into two separate components corresponding to sun and shade leaves (see e.g. Meister *et al*., 1987; Norman, 1992). This separation appears to be an over-simplification in the case of the sclerophyllous evergreen *Q. ilex*, as continuous modifications of anatomical and biochemical parameters have been recorded throughout the canopy (Rambal *et al*., 1996). Coefficients of variation for the thickness of different tissues are markedly higher in *Q. ilex* than in other oak species (Ashton & Berlyn, 1994; Ziegenhagen & Kausch, 1995; Hunter, 1997). In this study, sun-leaf : shade-leaf ratios for the palisade and spongy mesophyll thicknesses were 3.36 and 2.31, respectively, whereas for deciduous tree species adapted to a sunny environment, the equivalent ratios were only 2.36 and 1.51 (Jackson, 1967). Ashton and Berlyn (1994) showed that the increase of leaf adaptability allowed the plants to cope better with drought stress and to improve net photosynthesis.

The sampling strategy allowed parameters to be measured over the whole range of variation of leaves within the canopy. Ranges of total thickness and of palisade mesophyll thickness across the canopy were higher than those measured by Wagner *et al*. (1991) on the same species in northern Italy. In both studies, variation of total thickness originated from variation in palisade mesophyll. For *Q. ilex* (Wagner *et al*., 1991) as for other oaks (Ziegenhagen & Kausch, 1995; Hunter, 1997), palisade mesophyll in sun leaves was composed of two to three layers of cells, whereas in shade leaves it was composed of a single layer. Studying *Q. ilex* in Greece, Christodoulakis & Mitrakos (1987) found two palisade layers representing 52 % of the thickness of the leaf. This multi-layer structure of the palisade mesophyll of sun leaves may allow a higher photosynthetic rate (Parkhurst, 1986), as the columnar palisade cells act as light conduits that propagate light deeper into the mesophyll, thus distributing photon flux more evenly throughout the leaf (Vogelman & Martin, 1993; Smith *et al*., 1997). The ratio of cuticle and upper epidermis thickness from sun to shade leaves was 2.33, close to that of spongy mesophyll. This is consistent with the results of Wagner *et al*. (1991) for *Q. ilex*. The increase in upper epidermis thickness is generally considered to be an adaptation to a high photon flux density (Wagner *et al*., 1991). The continuous anatomical variations throughout the canopy are accompanied by gradual changes in photosynthetic characteristics (Hollinger, 1989; Ellsworth & Reich, 1993) suggesting that the photosynthetic apparatus at different levels in the canopy is adapted to the prevailing light conditions (Rambal *et al*., 1996).

The measured values of LMA ranged from 85 to 269 g m^{-2}. This range is equivalent to that obtained by several authors for the same species in southern France, Spain and Italy (Rambal *et al*., 1996), indicating that the current data set could be considered as representative of the great phenotypic plasticity of *Q. ilex*. As already emphasized by Rambal *et al*. (1996), no significant relationship between mass-based N concentration and LMA was obtained. Interpreting the continuous changes of anatomical parameters within the canopy in the frame of optimization theory, Rambal *et al*. (1996) suggest that LMA is particularly sensitive to increased light availability and tends to follow time-averaged irradiance levels. The large variations in LMA and palisade mesophyll thickness we observed in *Q. ilex* leaves suggests that acclimation to irradiance is dominated by changes in foliar anatomy rather than in biochemistry, as reported for deciduous woody species (Niinemets *et al*., 1998). In this context, LMA could be used as an indicator of physiological activity and may contribute to a broader application of photosynthesis modelling at the community and landscape levels (Pierce *et al*., 1994).

Working on fresh peach and olive leaves, Baldini *et al*. (1997) found that leaf transmittance in the 800–1100 nm spectral region was related to the mesophyll water content and the lamina thickness. By studying relationships between pine canopy reflectance and physiological properties in the 350–850 nm spectral region, Carter (1998) found that the efficiency of reflectance near 700 nm as an indicator of assimilation rate is explained by its high sensitivity to leaf chlorophyll content. In the studies already mentioned, correlations between optical properties and physiological and anatomical properties could not lead to predictive equations. In these works, optical properties were measured in the visible, far-red and near-near-IR (800–1100 nm) regions. By contrast, studies considering reflectance in the near-IR region have shown that NIRS analysis could be already considered as an efficient method for predicting the biochemical content of fresh leaves (Curran *et al*., 1992; Lacaze & Joffre, 1994; Martin & Aber, 1994; Yoder & Pettigrew-Crosby, 1995). In agreement with these works, the present results indicate that for the sclerophyllous Mediterranean *Q. ilex*, near-IR reflectance spectra of fresh leaves contain information related to anatomical (tissue thickness, LMA) and biochemical parameters. Analysis of reflected light has allowed formulation of independent predictive equations for LMA and palisade mesophyll thickness. This is particularly interesting because, as pointed out by Witkowski &

Table 4. *Statistics for the calibration equation for nitrogen concentration* ($mg\ g^{-1}$)

PLS regression					
Math treatment	Spectral region/ Pre-treatment	SEC	r^2	SEP	Terms
2,10,10	400–2500 nm				
	None	0.56	0.93	1.0	7
	Detrend	0.62	0.91	1.0	6
	SNV	0.51	0.94	1.1	7
	1100–2500 nm				
	None	0.65	0.89	1.0	6
	Detrend	0.65	0.89	1.0	6
	SNV	0.48	0.95	0.9	7
	400–1100 nm				
	None	0.79	0.85	1.5	6
	Detrend	1.14	0.69	1.7	3
	SNV	1.30	0.59	1.8	2
0,2,2	400–2500 nm				
	None	1.30	0.56	1.9	3
	Detrend	1.10	0.68	1.6	4
	SNV	1.20	0.63	1.7	4
	1100–2500 nm				
	None	1.10	0.70	1.3	7
	Detrend	1.10	0.68	1.4	5
	SNV	1.10	0.70	1.4	6
	400–1100 nm				
	None	1.40	0.51	1.8	4
	Detrend	1.40	0.53	1.7	3
	SNV	1.30	0.58	1.6	3

Stepwise regression					
Math treatment	Spectral region/ Pre-treatment	SEC	r^2	SEP	Wavelengths
2,10,10	400–2500 nm				
	None	0.60	0.92	1.3	1660, 2052, 2092
	Detrend	0.57	0.93	1.3	1460, 2052, 2116, 2452
	SNV	0.57	0.93	1.1	1660, 1956, 2052, 2452
	1100–2500 nm				
	None	0.62	0.92	1.3	1660, 2052, 2092
	Detrend	0.57	0.92	1.3	1460, 2052, 2116, 2452
	SNV	0.57	0.93	1.1	1660, 1956, 2052, 2452
	400–1100 nm				
	None	1.05	0.77	1.5	424, 704, 952, 1016
	Detrend	0.95	0.80	1.4	696, 952, 1016
	SNV	1.01	0.78	1.6	424, 736, 952, 1016
0,2,2	400–2500 nm				
	None	1.32	0.63	1.7	504, 688
	Detrend	1.47	0.53	2.1	696
	SNV	1.28	0.65	1.9	504, 2052
	1100–2500 nm				
	None	1.70	0.38	2.5	1908, 1964
	Detrend	1.15	0.72	1.7	1660, 1684
	SNV	1.40	0.57	2.5	1428, 2388
	400–1100 nm				
	None	1.32	0.63	1.7	504, 688
	Detrend	1.47	0.53	2.1	696
	SNV	1.13	0.73	2.0	616, 624, 640, 664

Calibration sample set $n = 61$ (range 9.1–18.0; mean 13.9; SD 2.0), validation sample set $n = 31$ (range 9.2–17.8; mean 13.95; SD 2.6). Math treatment indicates the transformation of spectral data: the first number is the order of the derivative function, the second is the segment length (nm) over which the derivative was taken, and the third the segment length over which the function was smoothed. SEC, standard error of calibration. SEP, standard error of prediction. Terms, number of terms used in the PLS calibration model.

Lamont (1991), the two components of LMA, leaf density and leaf thickness may respond independently to resource gradients. Therefore, independent remote predictions of both LMA and tissue thickness should help us to better understand the tuning of foliar anatomical properties to the gradient of environmental resources (Niinemets *et al*., 1998).

It should be noted that when stepwise regression was used, the selected wavebands were generally in the near-IR region (Tables 3, 4, 5), and that the equation statistics were not significantly improved when using the visible and far-red regions. As already pointed out by Joffre *et al*. (1992) and Bolster *et al*. (1996), our results showed that the PLS method of calibration provided consistently better accuracy than stepwise methods. Theoretical chemometrics studies demonstrated that the stepwise regression predictor has deficient performance when there is collinearity in spectral data (Martens & Naes, 1989). Moreover, Grossman *et al*. (1996) have shown that band selection using stepwise regression does not appear to be based upon the absorption characteristics of the predicted chemical analyses. Using all the spectral information through multivariate analysis of derivative spectra allowed us to solve the collinearity problem by using a small number of orthogonal regressors, and to build efficient equations for LMA, thickness of tissues and N concentration. Establishing predictive calibration equations is a crucial step before a generalized use of this approach. Analysing a large number of samples encompassing the widest range of features analysed (biochemical, anatomical, physiological), without unnecessary duplication of similar samples, remains necessary to develop accurate calibration equations. As stated by Shenk and Westerhaus (1996), the importance of selecting samples that represent all forms of expected variation cannot be over-emphasized.

Using one sampling geometry where reflectance was measured at 45° with respect to the leaf surface, leaf biochemical and anatomical properties were accurately predicted from leaf reflectance. The next step must be to verify whether similar results can be obtained for the entire canopy where leaves are randomly arranged. Our study concerned a sclerophyllous evergreen tree, a predominant growth form of Mediterranean vegetation. However, other growth forms, such as deciduous trees, co-occur in these ecosystems (Damesin *et al*., 1998). The results of Lacaze & Joffre (1994) have already shown that biochemical information could be efficiently extracted from NIRS spectra of fresh leaves of *Quercus pubescens*, a deciduous Mediterranean species. This result suggests that high spectral-resolution (10 nm) airborne imaging spectrometry over Mediterranean forests could be used, as by Peterson *et al*. (1988) and Zagolski *et al*. (1996), for remote-estimating leaf parameters such as LMA, thickness, anatomy and N concentration, and for deriving spatialized information about functional processes in these ecosystems.

ACKNOWLEDGEMENTS

This research was supported by the MOST project of the Program Environment of DG XII of the European Union (Contract EV5V-CT92-0210) and developed in the framework of the Core project MELODY of the GCTE IGBP programme.

REFERENCES

Abrams MD, Kubiske ME. 1990. Leaf structural characteristics of 31 hardwood and conifer species in central Wisconsin: influence of light regime and shade-tolerance rank. *Forest Ecology and Management* **31**: 245–253.

Abrams MD, Kubiske ME. 1994. Relating wet and dry year ecophysiology to leaf structure in contrasting tree species. *Ecology* **75**: 123–133.

Araus JL, Alegre L, Tapia L, Calafell R, Serret, MD. 1986. Relationships between photosynthetic capacity and leaf structure in several shade plants. *American Journal of Botany* **73**: 1760–1770.

Ashton PMS, Berlyn GP. 1994. A comparison of leaf physiology and anatomy of *Quercus* (section *Erythrobalanus–Fagaceae*) species in different light environments. *American Journal of Botany* **81**: 589–597.

Baldini E, Facini O, Nerozzi F, Rossi F, Rotondi A. 1997. Leaf characteristics and optical properties of different woody species. *Trees* **12**: 73–81.

Barnes RJ, Dhanoa MS, Lister SJ. 1989. Standard normal variate transformation and detrending of NIR spectra. *Applied Spectroscopy* **43**: 772–777.

Bolster KL, Martin ME, Aber JD. 1996. Determination of carbon fraction and nitrogen concentration in tree foliage by near infrared reflectance: a comparison of statistical methods. *Canadian Journal of Forest Research* **26**: 590–660.

Card DH, Peterson DL, Matson PA, Aber JD. 1988. Prediction of leaf chemistry by the use of visible and near infrared reflectance spectroscopy. *Remote Sensing of Environment* **26**: 123–147.

Carter GA. 1998. Reflectance wavebands and indices for remote estimation of photosynthesis and stomatal conductance in pine canopies. *Remote Sensing of Environment* **63**: 61–72.

Castro Diéz P, Villar Salvador P, Pérez Rontomé C, Maestro Martínez M, Montserrat Martí, G. 1997. Leaf morphology and leaf chemical composition in three *Quercus* (*Fagacae*) species along a rainfall gradient in NE Spain. *Trees* **11**: 127–134.

Christodoulakis NS, Mitrakos KA. 1987. Structural analysis of sclerophylly in eleven evergreen phanerophytes in Greece. In: Tenhunen JD, Catarino FM, Lange OL, Oechel WC, eds. *Plant response to stress*. NATO ASI Series, Vol. G15. Berlin, Germany: Springer-Verlag, 547–551.

Curran PJ. 1989. Remote sensing of foliar chemistry. *Remote Sensing of Environment* **30**: 271–278.

Curran PJ, Dungan JL, Macler BA, Plummer SE, Peterson DL. 1992. Reflectance spectroscopy of fresh whole leaves for the estimation of chemical concentration. *Remote Sensing of Environment* **39**: 153–166.

Damesin C, Rambal S, Joffre R. 1997. Between-tree variations in leaf $\delta^{13}C$ of *Quercus pubescens* and *Quercus ilex* among Mediterranean habitats with different water availability. *Oecologia* **111**: 26–35.

Damesin C, Rambal S, Joffre R. 1998. Co-occurrence of trees with different leaf habit: a functional approach of mediterranean oaks. *Acta Oecologica* **19**: 195–204.

Ellsworth DS, Reich PB. 1993. Canopy structure and vertical patterns of photosynthesis and related leaf traits in a deciduous forest. *Oecologia* **96**: 169–178.

Field C. 1991. Ecological scaling of carbon gain to stress and resource availability. In: Mooney HA, Winner WE, Pell EJ,

eds. *Response of plants to multiple stresses*. San Diego, CA, USA: Academic Press, 35–65.

Field C, Mooney HA. 1986. The photosynthesis–nitrogen relationship in wild plants. In: Givnish TD, ed. *On the economy of plant form and function*. Cambridge, UK: Cambridge University Press, 25–55.

Foley WJ, McIlwee A, Lawler I, Aragones L, Woolnough AP, Berding N. 1998. Ecological applications of near infrared reflectance spectroscopy – a tool for rapid, cost-effective prediction of the composition of plant and animal tissues and aspects of animal performance. *Oecologia* **116**: 293–305.

Givnish TJ. 1988. Adaptation to sun and shade: a whole-plant perspective. *Australian Journal of Plant Physiology* **15**: 63–92.

Grossman YL, Ustin SL, Jacquemoud S, Sanderson EW, Schmuck G, Verdebout J. 1996. Critique of stepwise multiple linear regression for the extraction of leaf biochemistry information from leaf reflectance data. *Remote Sensing of Environment* **56**: 182–193.

Gutschick VP, Wiegel FW. 1988. Optimizing the canopy photosynthesic rates by patterns of investment in specific leaf mass. *American Naturalist* **132**: 67–86.

Hanson HC. 1917. Leaf structure as related to environment. *American Journal of Botany* **4**: 533–560.

Hollinger DY. 1989. Canopy organisation and foliage photosynthetic capacity in a broad-leaved evergreen montane forest. *Functional Ecology* **3**: 53–62.

Hruschka WR. 1987. Data analysis: wavelength selection methods. In: Williams PC, Norris K, eds. *Near-infrared technology in the agriculture and food industries*. St Paul, USA: American Association of Cereal Chemists, 35–55.

Hunter JC. 1997. Correspondence of environmental tolerances with leaf and branch attributes for six co-occurring species of broadleaf evergreen trees in northern California. *Trees* **11**: 169–175.

Jackson LW. 1967. Effect of shade on leaf structure of deciduous tree species. *Ecology* **48**: 498–499.

Joffre R, Gillon D, Dardenne P, Agneessens R, Biston R. 1992. The use of near-infrared reflectance spectroscopy in litter decomposition studies. *Annales des Sciences Forestières* **49**: 481–488.

Johnson LF, Hlavka CA, Peterson DL. 1994. Multivariate analysis of AVIRIS data for canopy biochemical estimation along the Oregon transect. *Remote Sensing of Environment* **47**: 216–230.

Lacaze B, Joffre R. 1994. Extracting biochemical information from visible and near-infrared reflectance spectroscopy of fresh and dried leaves. *Journal of Plant Physiology* **144**: 277–281.

Mahalanobis PC. 1936. On the generalized distance in statistics. *Proceedings of the National Institute of Sciences*, *India* **2**: 49–55.

Martens H, Jensen SA. 1982. Partial least squares regression: a new two-stage NIR calibration method. In: Holas J, Kratchovil R, eds. *Proceedings of the 7th World Cereal Bread Congress*. Amsterdam, The Netherlands: Elsevier, 607–647.

Martens H, Naes T. 1989. *Multivariate calibration*. Chichester, UK: Wiley.

Martin ME, Aber JD. 1994. Analysis of forest foliage. III. Determining nitrogen, lignin and cellulose in fresh leaves using near infrared reflectance data. *Journal of Near Infrared Spectroscopy* **2**: 25–32.

McLellan TM, Martin ME, Aber JD, Melillo JM, Nadelhoffer KJ, Dewey B. 1991. Comparison of wet chemistry and near infrared reflectance measurements of carbon fraction chemistry and nitrogen concentration of forest foliage. *Canadian Journal of Forest Research* **21**: 1689–1694.

Meister HP, Caldwell MM, Tenhunen JD, Lange OL. 1987. Ecological implications of sun/shade-leaf differentiation in sclerophyllous canopies: assessment by canopy modeling. In: Tenhunen JD, Catarino FM, Lange OL, Oechel WC, eds. *Plant response to stress*. NATO ASI Series, Vol. G15. Berlin, Germany: Springer-Verlag, 401–411.

Meuret M, Dardenne P, Biston R, Poty O. 1993. The use of NIR in predicting nutritive value of Mediterranean tree and shrub foliage. *Journal of Near Infrared Spectroscopy* **1**: 45–54.

Niinemets Ü, Kull O, Tenhunen JD. 1998. An analysis of light effects on foliar morphology, physiology, and light interception in temperate deciduous woody species of contrasting shade tolerance. *Tree Physiology* **18**: 681–696.

Norman JM. 1992. Scaling processes between leaf and canopy levels. In: Elheringer JR, Field CB, eds. *Scaling physiological processes : leaf to globe*. San Diego, CA, USA: Academic Press, 41–76.

Norris KH, Barnes RF, Moore JE, Shenk JS. 1976. Predicting forage quality by infrared reflectance spectroscopy. *Journal of Animal Science* **43**: 889–897.

Oren R, Schulze ED, Matyssek R, Zimmerman R. 1986. Estimating photosynthetic rate and annual carbon gain in conifers from specific leaf weight and leaf biomass. *Oecologia* **70**: 187–193.

Parkhurst DF. 1986. Internal leaf structure: a three-dimensional perspective. In: Givnish TJ, ed. *On the economy of plant form and function*. Cambridge, UK: Cambridge University Press, 215–249.

Peterson DL, Aber JD, Matson PA, Card DH, Swanberg NS, Wessman C, Spanner M. 1988. Remote sensing of forest canopy and leaf biochemical contents. *Remote Sensing of Environment* **24**: 85–108.

Pierce LL, Running SW, Walker J. 1994. Regional-scale relationships of leaf area index to specific leaf area and leaf nitrogen content. *Ecological Applications* **4**: 313–321.

Rambal S. 1999. Spatial and temporal variations in productivity of Mediterranean-type ecosystems: a hierarchical perspective. In: Mooney HA, Saugier B, Roy J, eds. *Terrestrial global productivity : past*, *present*, *future*. San Diego, CA, USA: Academic Press. (In press.)

Rambal S, Damesin C, Joffre R, Méthy M, Lo Seen D. 1996. Optimization of carbon gain in canopies of Mediterranean evergreen oaks. *Annales des Sciences Forestières* **53**: 547–560.

Reich PB, Walters MB, Ellsworth DS. 1997. From tropics to tundra: global convergence in plant functioning. *Proceedings of the National Academy of Sciences*, *USA* **94**: 13730–13734.

Shenk JS, Westerhaus MO. 1991a. Population definition, sample selection, and calibration procedures for near-infrared reflectance spectroscopy. *Crop Science* **31**: 469–474.

Shenk JS, Westerhaus MO. 1991b. *ISI NIRS-2. Software for near-infrared instruments*. Silverspring, MD, USA: Infrasoft International.

Shenk JS, Westerhaus MO. 1996. Calibration the ISI way. In: Davies AMC, Williams PC, eds. *Near infrared spectroscopy : the future waves*. Chichester, UK: NIR Publications, 198–202.

Smith WK, Vogelman TC, DeLucia EH, Bell DT, Shepherd KA. 1997. Leaf form and photosynthesis. *BioScience* **47**: 785–793.

Specht RL, Specht A. 1989. Canopy structure in *Eucalyptus*-dominated communities in Australia along climatic gradients. *Oecologia Plantarum* **10**: 191–213.

Terashima I, Hikosaka K. 1995. Comparative ecophysiology of leaf and canopy photosynthesis. *Plant Cell Environment* **18**: 1111–1128.

Turrell FM. 1936. The area of the internal exposed surface of dicotyledon leaves. *American Journal of Botany* **23**: 255–263.

Vanderbilt VC, Grant L, Biehl LL, Robinson BF. 1985. Specular, diffuse, and polarized light scattered by two wheat canopies. *Applied Optics* **24**: 2408–2418.

Vogelmann TC, Martin G. 1993. The functional significance of palisade tissue: penetration of directional versus diffuse light. *Plant Cell Environment* **16**: 65–72.

Vogelmann TC, Nishio JM, Smith WK. 1996. Leaves and light capture: light propagation and gradients of carbon fixation within leaves. *Trends in Plant Sciences* **1**: 65–71.

Wagner J, Pelaez Menendez S, Larcher W. 1991. Bioclima e potenziale di produttività di *Quercus ilex* L. al limite settentrionale dell'areale di distribuzione. Parte III. Addattamento morfologico e funzionale delle foglie alle radiazioni luminose. *Studi Trentini Scienze Naturali* **68**: 37–51.

Wessman CA, Aber JD, Peterson DL. 1989. An evaluation of imaging spectometry for estimating forest canopy chemistry. *International Journal of Remote Sensing* **10**: 1293–1316.

Wessman CA, Aber JD, Peterson DL, Melillo JM. 1988. Remote sensing of canopy chemistry and nitrogen cycling in temperate forest ecosystems. *Nature* **335**: 154–156.

Windham WR, Mertens DR, Barton FE. 1989. Protocol for NIRS calibration: sample selection and equation development and validation. In: Marten GC, Shenk JS, Barton FE, eds. *Near infrared reflectance spectroscopy : analysis of forage quality*. Agricultural Handbook 643. Washington, USA: USDA-ARS, 96–103.

Witkowski ETF, Lamont BB. 1991. Leaf specific mass confounds leaf density and thickness. *Oecologia* **88**: 486–493.

Yoder BJ, Pettigrew-Crosby RE, 1995. Predicting nitrogen and chlorophyll content and concentration from reflectance spectra (400–2500 nm) at leaf and canopy scales. *Remote Sensing of Environment* **53**: 199–211.

Zagolski F, Pinel V, Romier J, Alcayde D, Fontanari J, Gastellu-Etchegorry JP, Giordano G, Marty G, Mougin E, Joffre R. 1996. Forest canopy chemistry with high spectral resolution. *International Journal of Remote Sensing* **17**: 1107–1128.

Ziegenhagen B, Kausch W. 1995. Productivity of young shaded oaks (*Quercus robur* L.) as corresponding to shoot morphology and leaf anatomy. *Forest Ecology and Management* **72**: 97–108.